Applied Catalysis B: Environmental 138–139 (2013) 149–160

Contents lists available at SciVerse ScienceDirect

Applied Catalysis B: Environmental

journal homepage: www.elsevier.com/locate/apcatb

Dechlorination of tetrachloro-*o*-benzoquinone by ozonation catalyzed by cesium loaded metal oxides

Suresh Maddila, Venkata D.B.C. Dasireddy, Sreekanth B. Jonnalagadda*

School of Chemistry, University of KwaZulu-Natal, Westville campus, Chiltern Hills, Durban, 4000, South Africa

ARTICLE INFO

Article history:
Received 4 October 2012
Received in revised form 28 January 2013
Accepted 1 February 2013
Available online 21 February 2013

Key words:
3,4,5,6-Tetrachlorocyclohexa-3,5-diene-1,2-dione
Ozone
Cesium Oxide loaded
Alumina
Silica
Titania
2,3-Dioxosuccinic acid
Oxalic acid

ABSTRACT

Ozone initiated oxidation of tetrachloro-*o*-benzoquinone (3,4,5,6-Tetrachlorocyclohexa-3,5-diene-1,2-dione, TCCD) in aqueous system catalyzed by different loadings of cesium oxide supported on metal oxides namely; Al_2O_3, SiO_2 and TiO_2 was investigated. Catalyst materials were characterized using different surface techniques including Raman, FT-IR, BET, SEM, TEM, ICP, TPD and XRD. XRD showed that cesium is in three different phases on the surface of the catalysts; and SEM and SEM-EDX indicated that cesium is well dispersed on the surface of the supports. Catalyst testing was done employing varying ozone molar ratios from 1 to 3 in the oxygen stream in a semi-batch reactor. 2,3-Dichloro-4,5-dioxohex-2-enedioic acid (DCA) was an intermediate and 2,3-dioxosuccinic acid (DSA) and oxalic acid (OA) were the main oxidation by-products. The oxidation products were characterized and confirmed by IR, ^{1}H NMR and Mass spectral data. The product distribution was dependent on the acidity of the supports. Among all the catalysts while 5% Cs/TiO_2 showed good activity, 1% Cs/SiO_2 showed relatively poor catalytic activity.

1. Introduction

Organochlorines are toxic and harmful due to their persistence, toxicity and capacity to accumulate in the living bodies [1]. Chlorination is one of the processes to inactivate the pathogenic microorganisms in aqueous environment, but it often initiates the formation of less oxidizable or more toxic by-products than the parent compounds [2]. Chlorine reacts with naturally occurring organic matter it forms chlorinated by-products such as chloroform, bromoform, haloacetic acids, short-chain carboxylic acids, haloacetonitriles, haloketones, and chloropicrin [3]. Chlorinated organic compounds are widely used in the textile and electronic and other chemical based industries. In particular, chlorophenols show low biodegradability and are persistent pollutants [4] posing serious problems to the environment once discharged into natural or waste waters. The toxicity of these compounds to humans and aquatic life imposes a high priority on their destruction in water. Biological treatment processes for the degradation of phenol and chlorophenols have usually proved to be inefficient due to their refractory nature [5]. Disposal of chlorinated organic waste in such a way as to minimize the environmental hazard has become an urgent issue. Conventional incineration of these waste produces harmful compounds such as pesticides, mono- and polycyclic aromatic hydrocarbons, chloro aromatic compounds, polychlorinated biphenyls (PCBs) as well as many phosphorous- and sulphur-containing compounds, unless the operating temperature is strictly controlled [6,7]. Dechlorination is an effective alternative procedure for decomposing chlorinated organic wastes under relatively mild conditions without the formation of the toxic by-products.

Ozone is one of the most effective oxidants which have been widely used in water and wastewater treatment. Ozonation is preferred to the chlorination and is frequently adopted to remove the herbicides from drinking water [8], without potential risk introducing chlorinated organics. Ozonation of the halogenated organic compounds in aqueous media have been studied by many researchers who have reported that the formation of bromate as a by-product is minimized by ozonation (pH < 7) [9,10]. Ozone is a popular disinfectant because it is effective for killing microorganisms and it significantly reduces the formation of halogenated DBPs, with the exception of water sources containing high halogen levels [11–14]. Ozonation has some advantages over chlorination like; it does not require additional processes to remove excess bactericidal agents from water hence higher doses of ozone can be used. A number of organic pollutants in aqueous environment such as phenols, amides, aromatics and halogenated derivatives are decomposed by ozonation by

* Corresponding author at: School of Chemistry & Physics, University of KwaZulu-Natal, Westville campus, Chiltern Hills, Durban-4000, South Africa.
Tel.: +27 31 260 7325; fax: +2731 260 3091.
E-mail address: jonnalagaddas@ukzn.ac.za (S.B. Jonnalagadda).

0926-3373/$ – see front matter © 2013 Elsevier B.V. All rights reserved.
http://dx.doi.org/10.1016/j.apcatb.2013.02.017

producing other oxygenated organic products (aldehydes, ketones and short-chain carboxylic acids), which are in more biodegradable [12,15,16]. Also ozonation produces complete mineralization of 3,4,5,6-Tetrachlorocyclohexa-3,5-diene-1,2-dione [17]. These DBPs constitute a large fraction of the assimilable organic carbon that can contribute to bacterial regrowth [18,19], because of this, many ozone drinking water plants use biological filtration to remove assimilable organic carbon before the finished water enters the distribution system.

To improve the performance of ozonation, ozone-based advanced oxidation processes (AOPs) such as O_3/UV, O_3/H_2O_2, $O_3/^{\bullet}OH$, O_3/UV/TiO_2 and homogeneous or heterogeneous catalytic ozonation have been reported and using for the oxidation of several organic compounds, pesticides and water treatments [20,21]. The decomposition of trichloroethene by ozone-adsorbed silica/zeolites has been reported due to their high stability than ozone existing in water [22]. Depending on the type of catalyst and organic moiety the adsorption of diffusion of organics on the surface of the catalysts or the concentrations of $^{\bullet}OH$ radicals produced on the solid/liquid interface is considered to be main responsible for the improvement of ozonation induced by the catalysts [23]. The effectiveness of ozonation depends on the nature of the catalyst, pH of the solution and ozone decomposition reactions. Metal oxide supported catalysts shows high activity on the surface and is higher than that of the metal supported catalyst on the gaseous phase. Metal oxides are widely used as heterogeneous catalyst for various controlled oxidation processes. Metal oxide supported catalysts are active in a wide range of applications, such as selective oxidations of several alkanes and alkenes, reduction of nitrogen oxides to ammonia. Metal-titania/alumina catalysts prepared by sol–gel procedures were studied as heterogeneous catalysts for the liquid phase oxidation of limonene and of NO_X emissions from stationary sources [24].

3,4,5,6-Tetrachlorocyclohexa-3,5-diene-1,2-dione (TCCD), which is commonly known as tetrachloro-*o*-benzoquinone is a brown colored compound with low water solubility and binds to soil as well in sediment. TCCD is widely used in the production of dyes and pigments and in tyre manufacturing. It is mainly also used in the synthesis of agrochemicals and textile/wool/leather dyeing and finishing. When it enters the aquatic and other environment, in soils, TCCD is not easily broken down by soil organisms, but absorbed by aquatic plants and animals which have the ability to store and concentrate the substances in their fatty tissues [16]. Many chlorinated organic do not have any strong nucleophilic sites, hence they are not easily prone to oxidation. Furthermore, oxidative degradation process could lead to some products which are more toxic than the original contaminants [18]. Thus the nature of products formed due to the ozone oxidation of TCCD is needed to be evaluated. The present study focuses on the ozone initiated oxidation of TCCD, catalyzed by cesium loaded metal oxides on alumina, silica and titania supports.

2. Experimental

2.1. Ozonalysis experiment

Ozone was generated using a Fischer Ozone 500 generator, which produced ozone by the electric discharge of oxygen from a compressed oxygen cylinder via the corona discharge method. Ozone gas was bubbled into a 50 cm^3 reactor through a sintered porous diffuser with porosity 2. All the ozone aeration experiments were carried out under the controlled conditions of room temperature (20 ± 1) °C at a flow rate of 1.0 L per min (LPM) and using 20 mL 10% v/v of tetrachloro-*o*-benzoquinone (TCCD) in water at fixed ozone concentration and flow rate for 5 h, un less otherwise specified. Fig. 1 illustrates the dimensions of the semi-batch reactor used. A magnetic stirrer placed at the bottom of the reaction vessel was used to ensure maximum contact of the substrate with ozone by continuous stirring. The amount of ozone was estimated by volumetric method trapping it in KI solution and titrating the liberated iodine using standard thiosulfate solution with starch as indicator [25]. Flow rates and ozone concentrations were calibrated and highly reproducible. Parameters were checked in duplicate runs, prior to and after each of the experiments. Results were highly reproducible and with less than 5% difference. Where difference was greater, such experiments replicated and data with less than 5% differences were only considered. As most of the experiments were done only in duplication, statistical analysis of the results could not be undertaken. In all cases although differences were small, trends were consistent, hence cautions approach is taken while comparing the results.

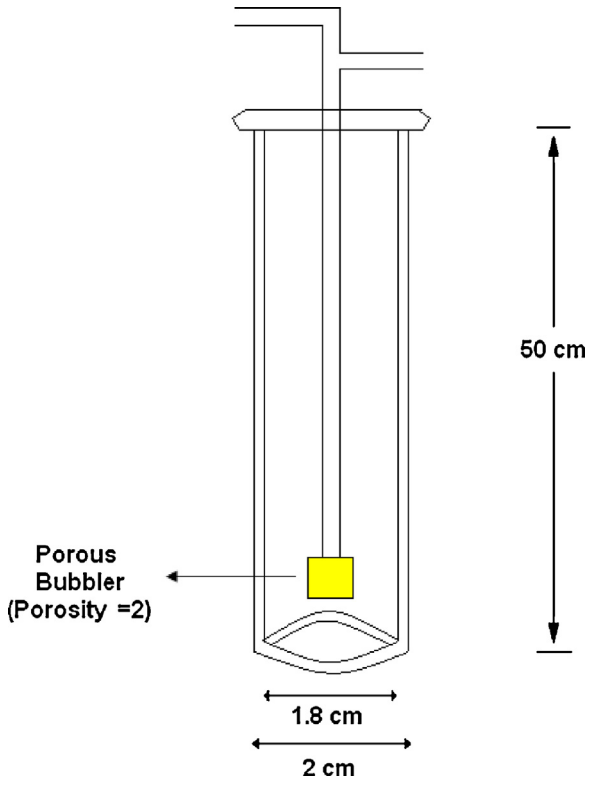

Fig. 1. Dimensions of reactor used in ozonation reactions.

The wet impregnation method was used in the preparation of metal oxide supported catalysts. The catalysts were prepared by wet impregnation method by dissolving appropriate amount of cesium nitrate in distilled water (20.0 mL) and adding it to 10 g of γ-Alumina (γ-Al_2O_3, Aldrich), Titania (TiO_2, Aldrich) and Silica (SiO_2, Aldrich) stirring for 3 hrs using a magnetic stirrer at room temperature and again at room temperature for overnight [26]. Catalysts are further dried in an oven at 130–140 °C for 12 h. Then the catalysts are calcined in the presence of air, at 550 °C for 3 h to obtain the 1% and 5% w/w catalysts [27,28].

3. Instrumentation

The BET surface areas were determined using a Micrometrics Gemini 2360 multi-point BET surface area analyser. The powdered samples (~0.05 g) were degassed overnight at 200 °C using a Micromeritics FlowPrep 060 instrument. The FT-IR spectroscopy of catalyst samples was carried out on a PerkinElmer BX model spectrometer in the 400–4000 cm^{-1} region. The Inductively

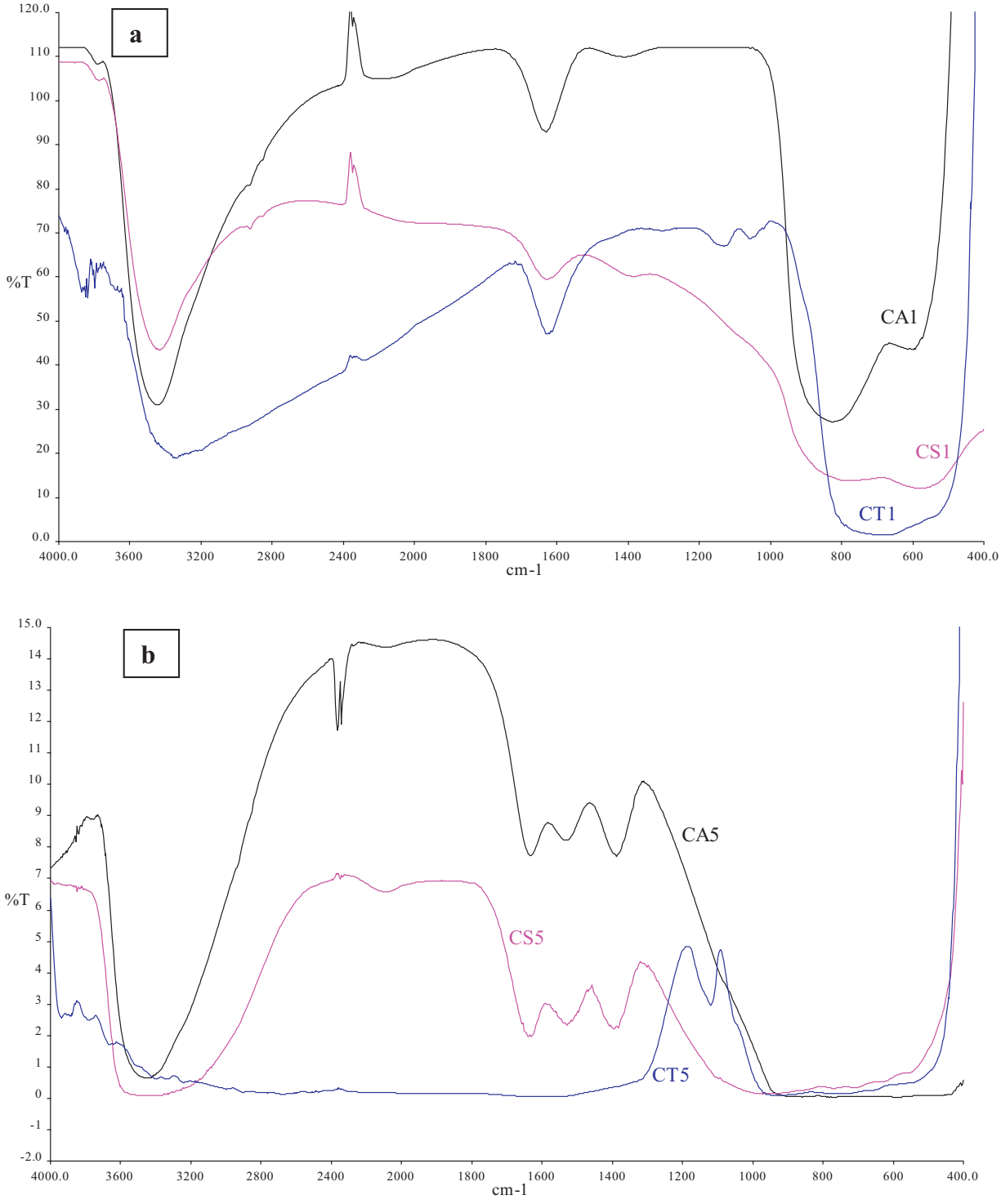

Fig. 2. Infrared Spectra of Cs loaded on Al_2O_3, SiO_2 and TiO_2 supports. (a) 1% Cs loaded and (b) 5% Cs loaded.

coupled plasma (ICP) was performed using a PerkinElmer Optical Emission Spectrometer Optima 5300 DV to determine the elemental composition of the materials and adsorption of the Cs on the three support materials. The SEM images were viewed in a Phillips XL30 Electron Scanning Microscope. Transmission electron microscopy (TEM) images were viewed using a Jeol JEM-1010 Electron Microscope. The images were captured and analyzed using iTEM software. X-ray diffraction patterns were recorded with Bruker D8 Advance instrument. The data was collected over the range 10–90° with a step size of 0.5 per second. The GC-MS analysis was carried out with ionization of electronic impact, 70 eV and the spectra were recorded in the interval 35–500 amu. It was equipped with a quadruple Agilent 5973 mass selective detector. Ammonia temperature programmed desorption (TPD) was carried out a Micromeritics 2920 Autochem II chemisorption analyser. In the TPD experiments, the temperature was set to 950 °C with a ramping rate at 10 °C/min using the flow of helium as the carrier gas. ^{1}H NMR (400 MHz), spectra were recorded on a Bruker AMX

400 MHz NMR spectrometer in $CDCl_3$/DMSO-d_6 solution using TMS as an internal standard. The mass spectra were recorded on Agilent 1100 LC/MSD instrument with method API–ES at 70 eV. All chemical shifts are reported in δ (ppm) using TMS as an internal standard.

4. Results and discussion

4.1. BET surface area and elemental analysis (BET)

ICP showed the nominal amount of cesium is present in the catalysts. All the catalysts showed type-IV H^1 isotherm, which shows the mesoporus nature of the catalysts (Supplementary materials Fig. 1). Surface area of the supports decreased with the cesium loading. This could be attributed to the clogging of the narrow pores of the support with the cesium making it inaccessible to nitrogen molecules, leading to a decrease in the surface area [29]. Cs loaded on Al_2O_3 and TiO_2 support material exhibited a lower surface area than silica supported catalysts. Surface area decreased with 5% loading of Cs on Al_2O_3, SiO_2 and TiO_2. The surface areas for the catalysts are shown in Table 1. The texture of the catalysts was dependent on the Cs concentration and the progressively high loadings resulted in a drastic decrease of the surface area as well as the pore volume.

4.2. Fourier transform infrared spectroscopy (FT-IR)

A distinct IR absorption bands at 1413 and 1388 cm^{-1} observed with 1% and 5% Cs/Al_2O_3. Al_2O_3 peaks are overlapping with the Cs—O vibrational stretching arising from the presence of Cs_2O [30–32]. The stretching vibration of hydroxyl groups and also other peaks appeared at 1632 cm^{-1}, 2204 cm^{-1} and 3452 cm^{-1} for 1% Cs/Al_2O_3 and 2366 cm^{-1} and 3435 cm^{-1} which can be attributed to the adsorbed moisture on the surface of the catalyst (Fig. 2CA1, CA5) [28,30,31]. The FT-IR spectrum of pure silica shows bands due to tetrahedral framework vibrations of Si—O—Si linkages at 1098 and 801 cm^{-1}. As the Cs_2O loading increases to 1% and 5%, these characteristic bands shift systematically to lower wave numbers indicating that the loading of Cs, strengths the physisorbed forces between the metal and support can be noticed in (Fig. 2CS1, CS5). The bands at 1098 and 801 cm^{-1} in pure SiO_2 shift to 1055 and 791 cm^{-1} due to 1% Cs/SiO_2, 1090 and 788 respectively in Cs/SiO_2 sample. The vibrational stretching frequency of the hydroxyl group appears at 3436 and 3440 cm^{-1} same as Cs/Al_2O_3 shows the presence of moisture. The Si—O—Si bond which is observed at 1055 cm^{-1} and 1090 cm^{-1} is probably overlapping with the Cs/SiO_2 absorption bands. [30,31,33].

The absorption band at 1131 and 1120 cm^{-1} with 1% and 5% Cs/TiO_2 shows Cs—O vibrational stretching which can be attributed to the presence of Cs_2O. The two bands at 589 cm^{-1}, 797 cm^{-1} and 584 cm^{-1}, 801 cm^{-1} are due to presence of 1% and 5% TiO_2 [31–34]. The absorption bands at 1628 cm^{-1} and 3441 cm^{-1} 1% Cs/TiO_2 as well as 3462 cm^{-1} for 5% can be assigned to the hydroxyl group vibrational stretching. (Fig. 2CS1, CS5).

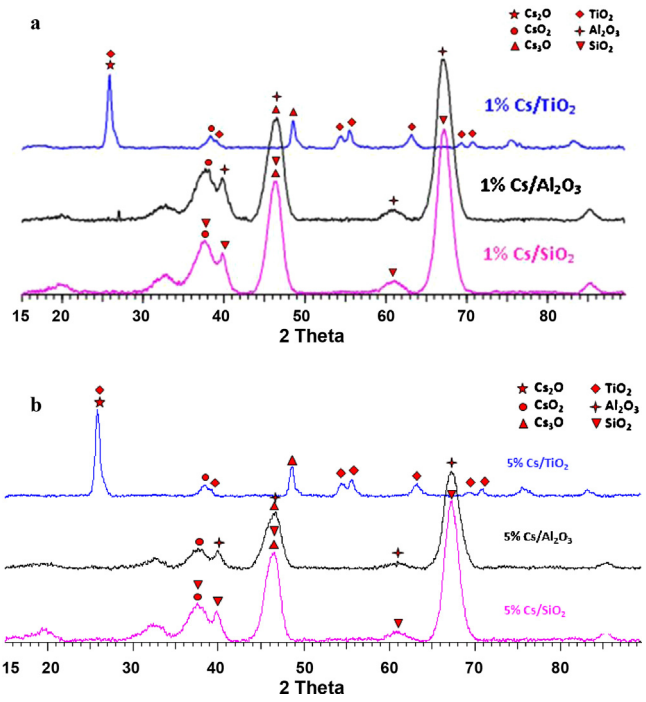

Fig. 3. XRD spectra: (a) 1% Cs loaded on Al_2O_3, SiO_2 and TiO_2 support. (b) 5% Cs loaded on Al_2O_3, SiO_2 and TiO_2 support.

4.3. X-ray diffraction (XRD)

The powder XRD diffraction patterns (Fig. 3a and b) of all the prepared catalysts show the presence of the CsO_2, Cs_3O and Cs_2O phases, with d-spacing values of 2.36, 1.88 and 3.43 Å for 2θ angles of 38, 48 and 26° respectively. The d-spacing phases are of the correlating with the ICDD File numbers are 03-065-2662, 01-085-0437 and 01-074-1918 for CsO_2, Cs_3O and Cs_2O phases respectively. The phases of supports i.e. alumina, silica and titania are correlating with literature [28]. The increase in the cesium loading was shown by slight peak shift in the XRD diffractogram. By increasing in cesium loading, there is no evidence of additional phase of cesium.

4.4. Scanning electron microscopy (SEM)

In the presence of Cs on Al_2O_3 surface is noticeable in Fig. 4a and becomes more conspicuous in Fig. 4b as it seems to totally occupy the pores as observed from Fig. 4c, Cs is distributed over silica surface. An increase to 5% Cs loading (Fig. 4d) showed that Cs particles are closer together and occupy the surface more densely consistent with BET results. From Fig. 4e, it is shown that Cs (white fluffy

Table 1
BET surface area, elemental analysis and TPD data of Cs loaded supports.

Catalyst (%)	Cs wt.% (ICP)	Surface Area (m^2/g)	Pore volume (cm^3/g)	Cs wt.% (EDX)	Acidity (mmol NH_3/g)	Specific acidity (mmol NH_3/m^2)
Al_2O_3	–	251	0.98	–	920	4.27
1% Cs/Al_2O_3	0.98	236	0.74	0.98	780	3.30
5% Cs/Al_2O_3	4.95	221	0.69	4.95	610	2.76
SiO_2	–	210	0.75	–	3600	20.00
1% Cs/SiO_2	0.95	208	0.56	0.95	2950	14.18
5% Cs/SiO_2	4.93	187	0.50	4.93	2241	11.98
TiO_2	–	83	0.42	–	620	13.80
1% Cs/TiO_2	0.99	73	0.28	0.99	591	8.09
5% Cs/TiO_2	4.97	69	0.25	4.97	578	8.37

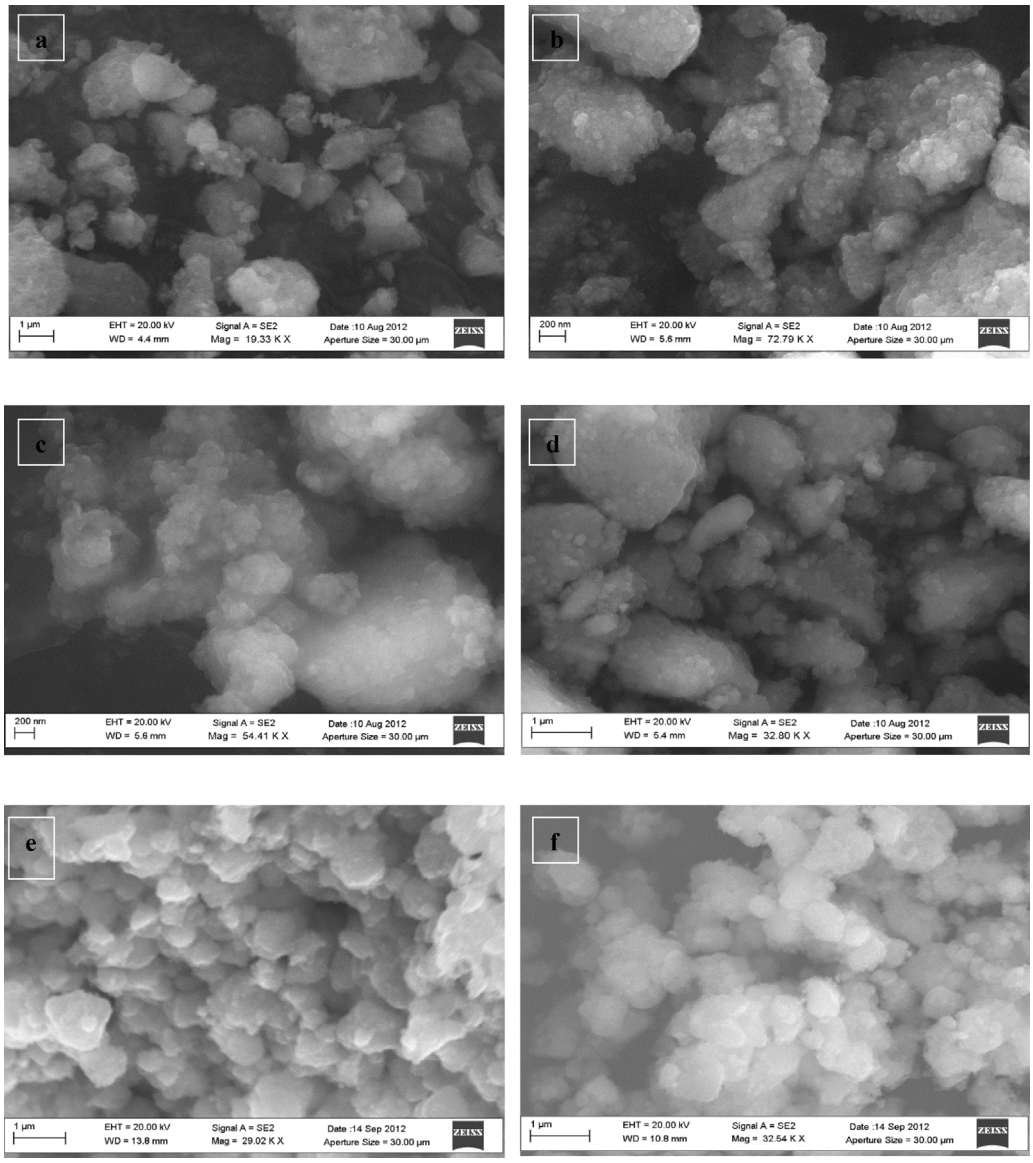

Fig. 4. SEM images: (a and b) 1% Cs and 5% Cs on Al_2O_3 support; (c and d) 1% Cs and 5% Cs on SiO_2 support; (e and f) 1% Cs and 5% Cs on TiO_2 support.

substance) is evenly dispersed on the surface of titanium dioxide. When Cs loading is increased to 5% (Fig. 4f), the pores of TiO_2 appear to be completely occupied. Wide distribution of small particles over support material is observed with 1% Cs loading. With an increase from 1 wt.% to 5 wt.% Cs loading, Al_2O_3 and TiO_2 surfaces seem to be completely occupied with Cs. For silica, the Cs particles are closer together but much of the surface is still visible. A possible reason could be that silica has a large surface area and therefore requires more Cs particles to occupy its pores. The SEM images confirm the crystalline nature of the catalysts, which is not affected by the different loadings of cesium. SEM-EDX shows that the cesium is evenly distributed on the surface of the supports, and SEM-EDX results are in correlation with ICP-OES elemental analysis (Table 1).

The TEM images of all the powders showed an agglomeration of particles. Agglomeration of particles is the result of exposure of the samples to a beam with the high energy resulting in the loss of hydroxyl groups. On high magnification, the particles appear as irregular a needle-like shape which was also observed in literature. The darker parts of the images show the presence of cesium dispersed evenly on the surface which appear as elongated rod-like particles in the TEM images with particle sizes around 50–100 nm (Fig. 5).

4.5. Temperature programmed desorption of ammonia (TPD-NH_3)

From the TPD experiments it is evidenced that the cesium decreases the acidic nature of the supports which is also recorded by decrease of specific acidity (Table 1). Cesium oxide, which is a strong base, with interaction with the acidic sites on the surface of the supports, i.e., silica, alumina and titania reduces their surface acidity. With silica acidic by nature, among all the catalysts, cesium supported on silica catalysts showed high acidity and specific acidity. Further, the decrease in the acidic nature is high with silica relative to the other supports with cesium loading. Thus the cesium loading is effecting mainly the Bronsted acidic sites (strong acidic) on the silica surface, but not diminishing the Lewis acidic sites (Weak acidic sites). Thus, by comparison of the decrease in the ratio of the acidity, we can perceive that cesium is diminishing the Bronsted acidic sties of the silica, but it is not affecting the Bronsted sites of the other supports i.e. alumina and titania.

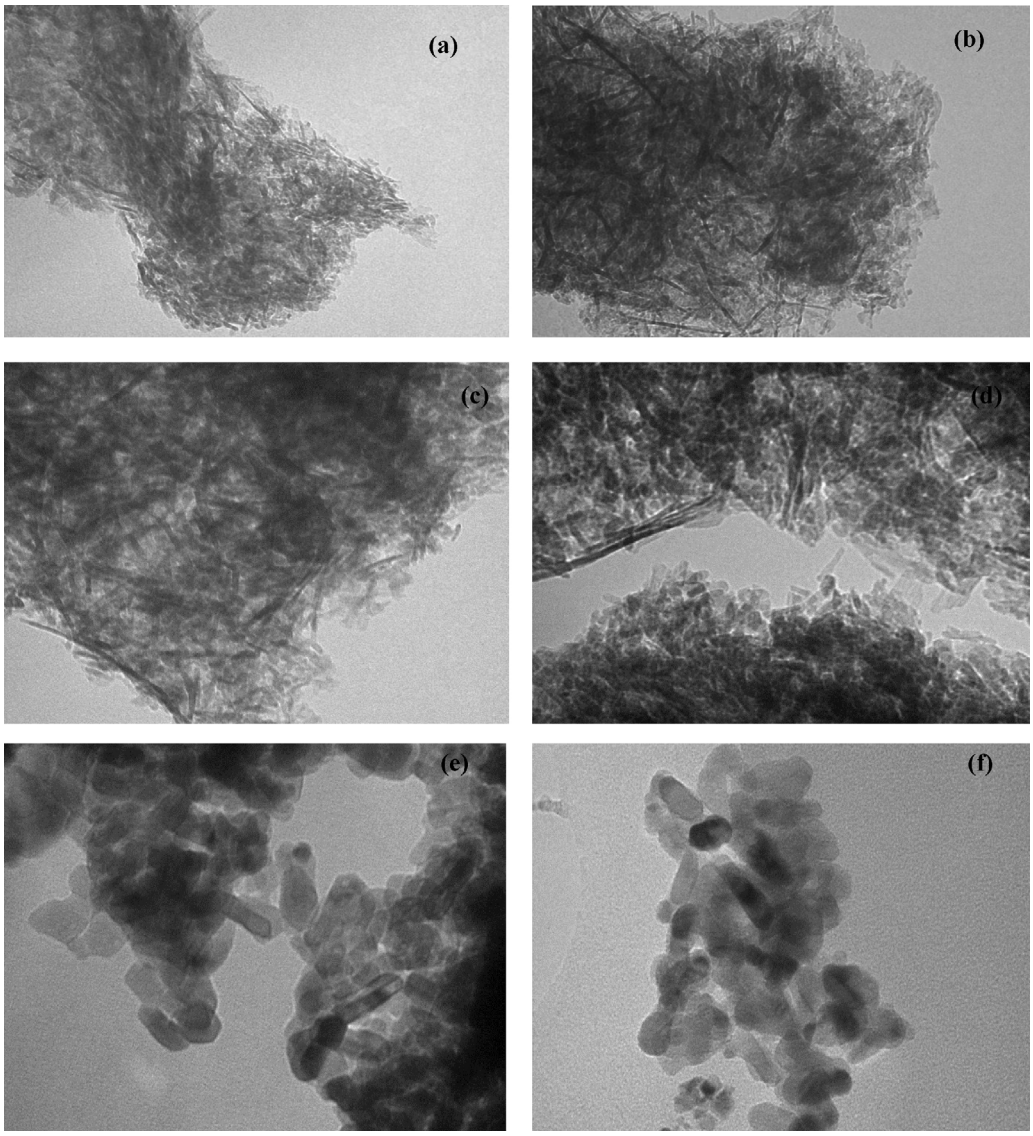

Fig. 5. TEM images: (a and b) 1% Cs and 5% Cs on Al_2O_3 support; (c and d) 1% Cs and 5% Cs on SiO_2 support; (e and f) 1% Cs and 5% Cs on TiO_2 support.

4.6. Catalyst testing and product identification

All ozonation reactions were done either in duplicate or in triplicate. Conversion and selectivity was calculated for all reactions. Initially, all the catalysts are tested with time at an ozone molar ratio of 2 until to get 100% conversion. All the ozonation experiments were conducted by aerating the samples with ozone enriched with oxygen for different molar ratios, in a range of 0.5–3.0. No reaction occurred with oxygen alone. After ozone aeration, the organic portion of the reaction mixture was extracted and analyzed the products at each reaction. One intermediate and two major products and during reaction progress for the reactions were separated and identified by GC/GC–MS (Fig. 6). Based on the mass spectra and the reference standards, the intermediate was confirmed to be 2,3-dichloro-4,5-dioxohex-2-enedioic acid (DCA) (Fig. 7), and main oxidation products were 2,3-dioxosuccinic acid (DSA) and oxalic acid (OA) (Supplementary materials Fig. 2a and b) The IR spectra of intermediate compound, DCA showed a characteristic absorption bands at 3460, 1624 and 783 cm^{-1} for the COOH, C=O and C—Cl stretching vibrations, respectively (Fig. 8). Its ^{1}H-NMR spectra showed a singlet for the two proton of the COOH group at δ 14.32 ppm respectively (Fig. 9). IR spectra of compound DSA exhibited characteristic absorption band ranges at 3599 cm^{-1}, 3410 cm^{-1} due to 2COOH and 1721, 1685 cm^{-1} due to 2C=O groups stretching respectively (Supplementary materials Fig. 3a). The ^{1}H-NMR spectra showed broad singlet at δ 12.51 ppm for 2COOH protons (Supplementary materials Fig. 3b). The IR spectra of compound OA exhibited characteristic absorption bands at 3448 cm^{-1}, 3247 cm^{-1}, and 1629 cm^{-1} corresponding COOH, COOH, and C=O stretching respectively (Supplementary materials Fig. 3c). Similarly the ^{1}H-NMR spectra displayed peaks due to in the range of broad singlet at δ 10.11 ppm for 2COOH protons (Supplementary materials Fig. 3d).

The functional groups observed in the IR and ^{1}H-NMR, Mass spectrum were in good agreement with spectra corresponding to DCA, DSA and OA. Further the qualitative test (lime water) confirmed the release of CO_2 during the ozonation reaction and suggesting the some mineralization of TCCD. Ozonation of organic compounds in water is known to produce more biodegradable oxygenated organic products and low molecular weight acids [35,36]. The $NaHCO_3$, 2,4-DNP test positively confirmed that products constitute some aldehydes, carboxylic acids or ketones [37]. The intermediate DCA is not bioaccumulative and is biodegradable [38].

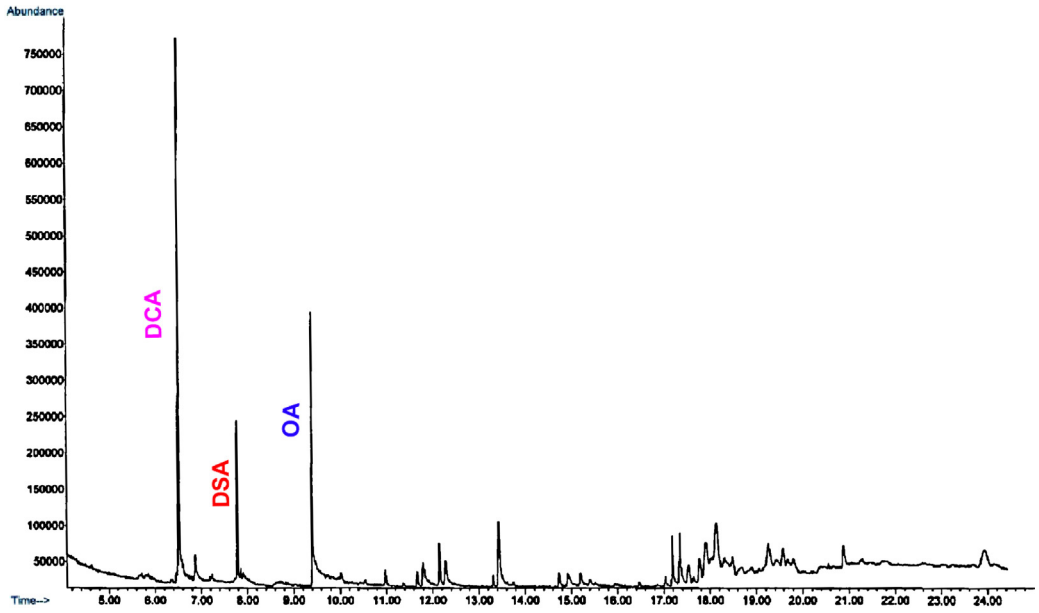

Fig. 6. GC–MS chromatogram of product mixture.

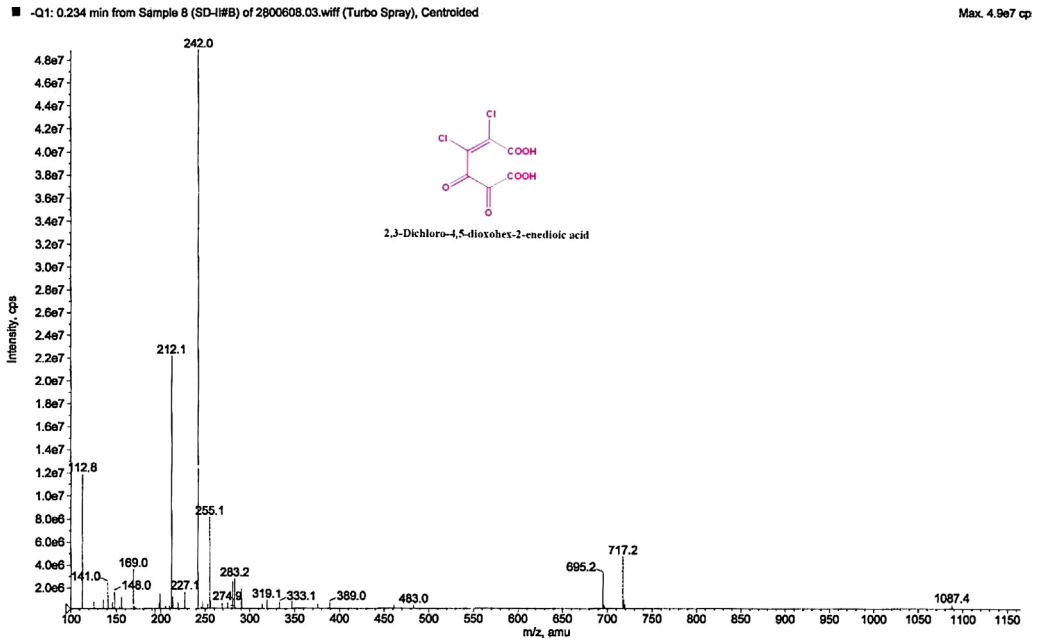

Fig. 7. Mass spectrum of 2,3-Dichloro-4,5-dioxohex-2-enedioic acid (DCA).

With prolonged ozonation, these products are further oxidized to oxalic acid.

4.6.1. Uncatalysed reactions

Conversion (%) of TCCD increased with increase in ozone concentration. A perusal of data in Table 2 shows an increase in conversion (%) of TCCD to DCA and DCA to DSA and OA, and to CO_2 with increasing ozone molar ratio and decrease in selectivity toward partially oxidized product, DCA. At higher O_3 ratios, the deep oxidation taking place which was indicated by the increase in the selectivity of oxalic acid and DSA and more mineralization.

4.6.2. Conversion and selectivity

The ozonation process at acidic, neutral and alkaline pH medium mainly takes place through the direct oxidation of specific

Table 2
Uncatalysed reaction with varying ozone ratios – conversion (%) and selectivity.[a]

O_3 Ratio	Conversion	Selectivity (mol%)[b]			
	(mol%)	DCA	DSA	OA	UnQ
0.5	16.2	95.1	3.2	1.7	>1.7
1.0	28.4	84.2	6.8	9.0	>6.8
1.5	35.6	73.5	7.4	19.1	>7.4
2.0	40.1	69.1	12.5	18.4	>12.5
2.5	45.3	63.2	23.8	13.0	>13.0
3.0	54.7	59.1	27.1	13.8	>13.8

[a] pH 7 and after 2 h ozonation.
[b] 2,3-dichloro-4,5-dioxohex-2-enedioic acid (DCA); 2,3-dioxosuccinic acid (DSA); oxalic acid (OA) and Un-Quantified CO_2 and H_2O (UnQ).

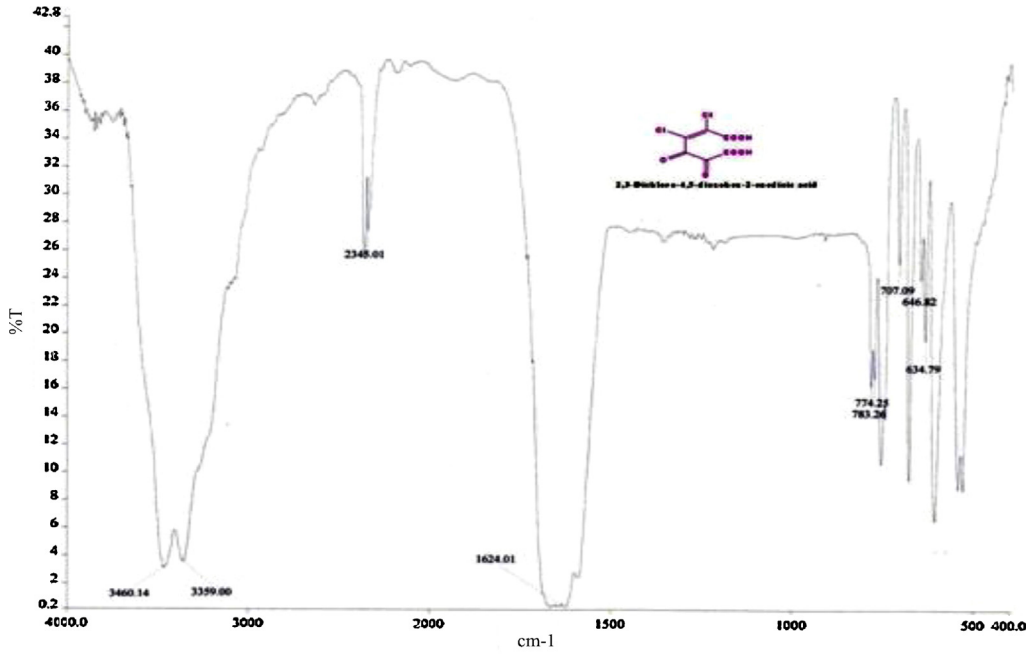

Fig. 8. Infrared Spectra of DCA.

functional groups by molecular ozone, which reacts selectively [39]. To optimize the pH of the reaction, ozonation experiments were conducted with 10% v/v of tetrachloro-*o*-benzoquinone, at pH 3, 5, 7, 9 and 11 in presence of 1% Cs loaded on three oxide supports (Table 3). Uncatalysed ozonation and with 1% Cs loaded supports were conducted at acidic, neutral and alkaline pH conditions (Table 3). Uncatalysed reaction recorded improved conversions with increasing pH, which suggests that hydroxyl radicals facilitate the faster oxidation under alkaline conditions [40]. A perusal of conversion (%) data in Table 3 indicates that unlike the uncatalysed reaction, optimum pH for TCCD degradation for all three catalysts is pH 7 as reaction at acidic and basic conditions recorded relatively lower conversions. No enhanced reactivity under alkaline conditions, suggest that broadly molecular O_3 was the main reactive species [41]. Hence, the further catalyzed ozonation studies were performed at neutral pH. The Table 3 also summarizes the data for conversion (%) of TCCD, and selectivity of products toward 1% Cs loaded on Al_2O_3, SiO_2 and TiO_2 at pH 3, 5, 7, 9 and 11 respectively. An examination of the results suggests that conversion (%) for the uncatalysed reaction at pH 7 showed good conversion relative to acidic and alkaline conditions. Further their conversion of TCCD was 70.1%, 60.0% and 50.2% respectively

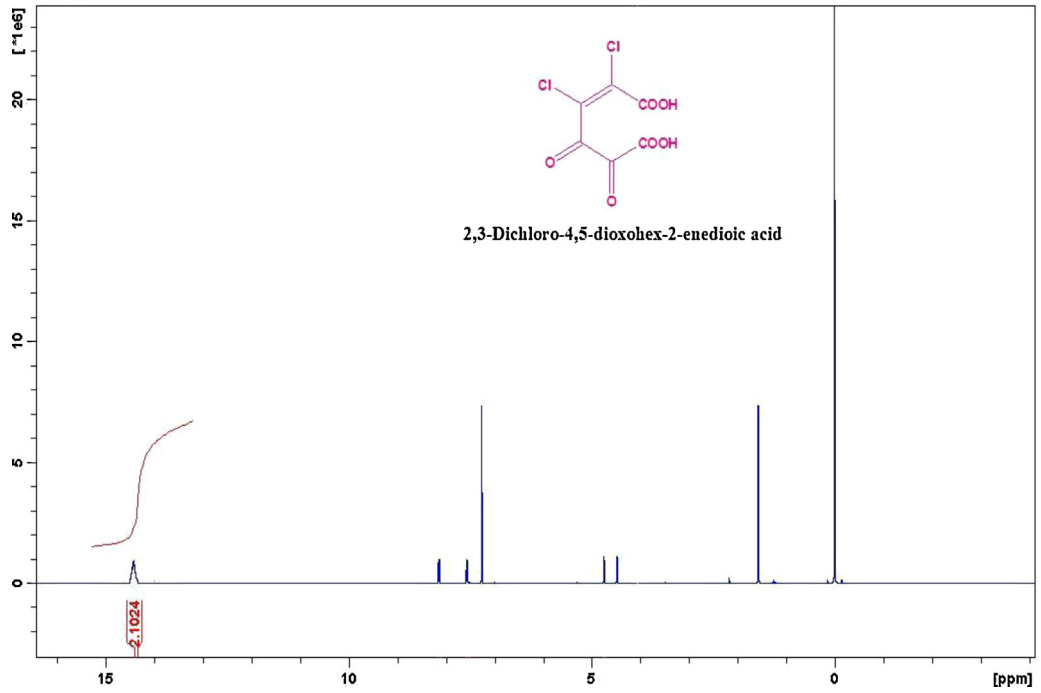

Fig. 9. ^{1}H NMR spectra of DCA.

Table 3
Conversion of TCCD ozonation with varying pH (1% w/w Cs loaded catalysts).

pH	Conversion (mol%)[a]			
	Uncatalyzed	1% Cs/Al_2O_3	1% Cs/SiO_2	1% Cs/TiO_2
3	16.2	28.0	23.6	34.0
5	28.4	45.8	41.8	52.5
7	35.6	60.0	50.2	70.1
9	40.1	50.2	48.6	46.8
11	45.3	38.4	36.9	35.9

[a] 2 h ozonation ozone molar ratio 1.5.

Table 4
Conversion (%) of TCCD with time.

Ozonation	Conversion (mol%)[a]			
Time/min	Uncatalyzed	1% Cs/Al_2O_3	1% Cs/SiO_2	1% Cs/TiO_2
30	15.1	27.1	21.8	26.8
60	28.3	36.8	30.5	34.1
90	35.4	44.9	36.4	44.7
120	40.1	52.1	44.2	55.3
150	46.8	64.2	51.7	68.7
180	54.7	73.4	62.7	81.5
210	57.1	87.1	78.7	93.7
240	59.8	92.4	83.8	100
270	65.4	100	96.4	100
300	69.1	100	100	100

[a] pH 7.0 and Ozone molar ratio 2.

with TiO_2, Al_2O_3 and SiO_2 as supports. The obtained results which indicate that neutral pH provides optimal conditions for both for the ozone decomposition and for catalyst activity. Concentration profiles of the TCCD conversion are the degradation period was shorter, caused by the effect of additional radical reactions.

4.6.3. Effect of ozonation duration on conversion (%) of TCCD

The results of conversion of TCCD for the uncatalysed ozonation and in presence of 1% Cs loaded on alumina, silica, titania as function of ozonation duration were investigated. A perusal of data in Table 4 show that after 60 min ozonation, the conversion (%) with Cs loaded metal oxides was higher compared to 28.3% with uncatalysed reaction, i.e. with alumina (36.8), silica (30.5) and titania (34.1). In every experiment obviously the conversion (%) increased with increased duration of ozonation. After 240 min ozonation, relative to uncatalysed (59.8%), catalysts had improved conversions, viz. Cs/alumina (92.4), Cs/silica (83.8), and Cs/titania (100). Cs/Alumina reached 100% after 270 min and Cs/Silica after 300 min ozonation. Interestingly, relative to uncatalysed ozonation, except titania, the conversion (%) was lower with other oxides materials alone, but the selectivity toward products varied significantly.

4.6.4. Effect of ozone molar ratio

Ozone, due to its conjugate structure, can react as a dipole, an electrophilic or a nucleophilic agent. As a result of its high reactivity, ozone is very unstable in water. The half-time of molecular ozone varies from a few seconds to minutes and depends on pH, water temperature and concentration of organic compounds in water [41]. Conversions of TCCD and selectivity toward different products for different ozone ratios for 1% Cs and 5% Cs loaded on the three supports are summarized (Supplementary materials Table 1). In addition to the relative % of DCA, DSA and OA, the % un-quantified product, which is mineralized (1 mol TCCD = 6 mol of CO_2) is also included. Similar to uncatalysed reactions, all the catalyzed reactions showed an increase in conversion (%) of TCCD with the increased ozone ratio. With the increase in ozone molar ratio in the reaction mixture, there was decrease in % conversion of DCA. The selectivity toward DCA was highest with 1% Cs/TiO_2 at an ozone molar ratio of 0.5 (Supplementary materials Table 1).

4.6.5. Effect of Cesium loadings

The cesium catalyzed reactions, showed that the conversion is dependent on the cesium loading on the surface of the support. As the cesium loading is increased, the percentage conversion of TCCD also increased with all the molar ozone ratios investigated (Supplementary materials Table 1). Observed increase can be attributed to the increased availability of the cesium oxide active sites on the surface. The higher activity of the metal impregnated catalysts can be due to enhanced ozone decomposition, compared to the supports itself. This probably results from the increase of electron transfer and an increase in the rate of oxidation which accelerates the catalytic reactions [28]. The surface area of the catalysts decreased with occupying the pores of the supports, which decreases the Bronsted acidity of the catalyst, which facilitates the oxidation capacity of the catalyst. Reactivity of cesium on support material could be due to the metal and support interaction as well as the consequential changes in the surface properties of the reactive sites, which facilitate the substrate adsorption to the active site and its subsequent oxidation directly by molecular ozone or the ozone decomposed on adjacent site. The active site can decompose ozone. The bond between metal and oxygen species is appropriately strong and the other bond is weak enough for oxidant species to react with other reactant. The increased activity is resultant of the factors like interaction of a metal with a catalyst support, and adsorption abilities of catalyst supports could affect the activity of a catalyst.

4.6.6. Effect of the supports

The results of percentage conversion and selectivity toward six catalysts with 1% and 5% Cs loaded on three metal oxide supports are summarized (Supplementary materials Table 1). The ozone molar ratios and conversion efficiencies with different loadings of Cs on metal oxide supports are illustrated in Fig. 10. The conversion (%) increased with increase in ozonation time, the ozone molar ratios and cesium loading on the support. Thus, with all supports, 0.5 molar ratio of ozone and 1% Cs loaded catalysts having a lower % conversion than the 5% loaded. The efficiency conversion was in the order with $TiO_2 > Al_2O_3 > SiO_2$ as supports, while the selectivity toward DCA in the reverse order, i.e. $SiO_2 > Al_2O_3 > TiO_2$. With 1% Cs loaded on SiO_2, Al_2O_3, and TiO_2 catalysts selectivity toward DCA was 90.3%, 85.6% and 75.4%, while with 5% Cs selectivity toward DCA was 81.9%, 71.9% and 72.4% respectively. As oxidation of both TCCD and DCA by ozone was facilitated by the catalyst with similar efficiency, DCA was also further converted to DSA and OA and to CO_2, thus decreasing the selectivity toward DCA. Observed selectivity of silica toward DCA is due its acidic nature and weak oxidative property [42].

An observation of the results presented (Supplementary materials Table 1) show that selectivity toward oxalic acid with 1% Cs on titania was relatively higher than toward DSA. While the selectivity toward DSA and OA varied from one catalyst to other, but for all % selectivity decreased toward DCA and increased toward OA and DSA with increasing ozone molar ratio, which facilitated further oxidation of DCA. The efficiency selectivity was in the order of $TiO_2 > Al_2O_3 > SiO_2$. The BET analysis of catalysts revealed that surface areas were in the order of Cs/Al_2O_3 > Cs/SiO_2 > Cs/TiO_2 (Table 1). Catalyst activity seems to be independent of catalyst surface area, as conversion and selectivity were of similar magnitude in all three cases, pointing that activity is resultant of the combination of active sites of cesium and support material.

The heterogeneous catalyst supports used are primarily metal oxides such as Al_2O_3, SiO_2 and TiO_2 [41]. The hydroxyl groups on the surfaces of the metal oxides behave as Bronsted acid sites

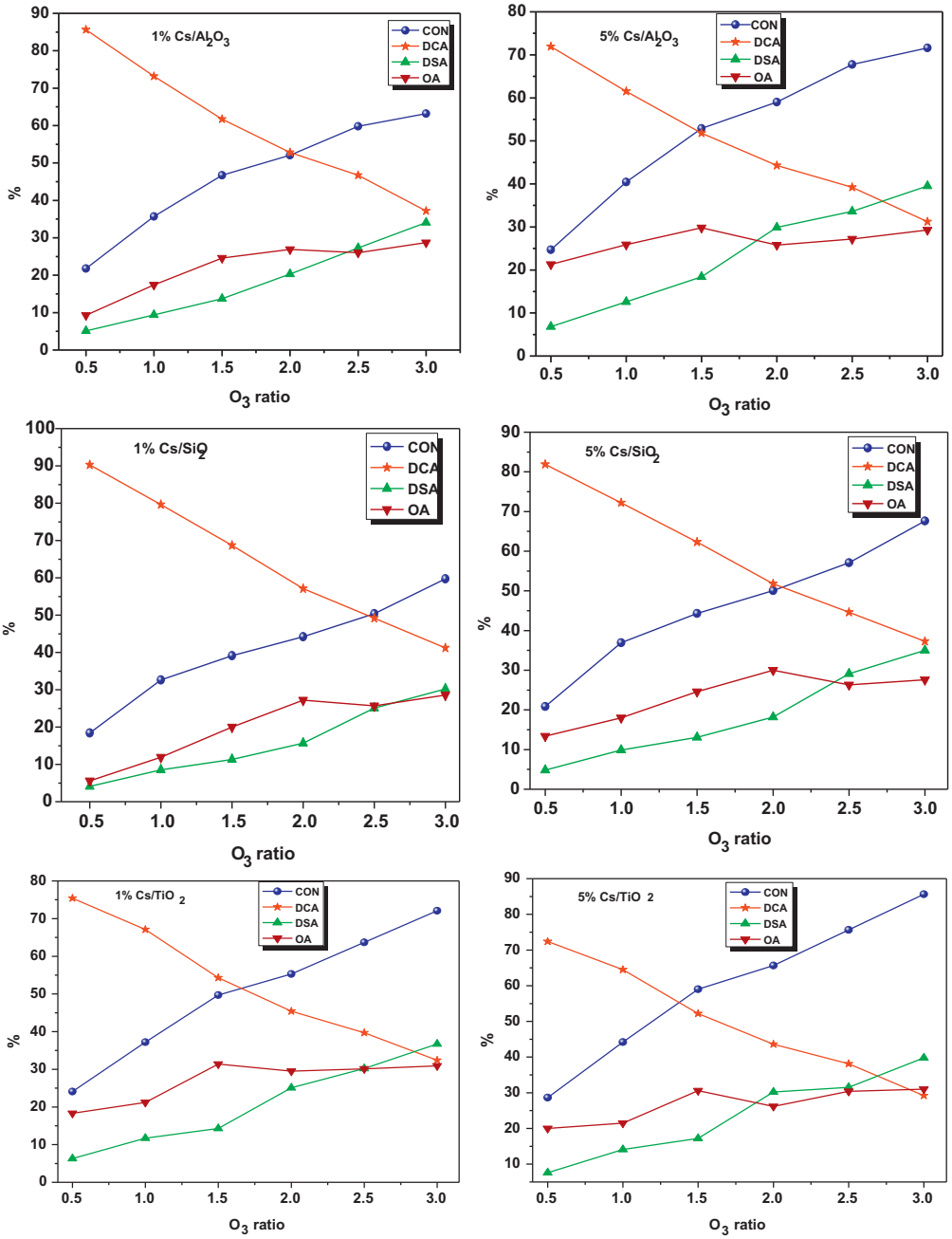

Fig. 10. The conversion and ozone molar ratios with 1% and 5% loadings of Cs on metal oxide supports.

(proton donors), whereas Lewis acid sites (electron pair acceptors) are located on the metal cation. Both Bronsted and Lewis acid sites on the cesium surface are thought to be the catalytic reaction centers and the hydroxyl radicals are typically generated from the transformation of dissolved ozone on the supports. The catalytic ozonation is expected to proceed at the reactive sites, which can lie inside and outside the surfaces [41].

The ozonation reactions over combinations of metal oxides have been explained by a spill-over mechanism. Oxygen is adsorbed and activated on one metal oxide (the donor) and transferred to the second metal oxide (the acceptor). The reactant (hydrocarbon) reacts with the oxygen adsorbed on the acceptor.

For Cs/SiO_2 catalysts prepared by wet impregnation methods, the number of acid sites decreased with increase in cesium loading [42]. On alumina, at low cesium coverage, a large part of the cesium layer is bound to acid–base pairs of alumina. The lattice oxygen mobility is improved by increasing the cesium loading which affects the catalytic activity. Deposition of cesium on alumina and titania supports lead to lower number of acid sites than the respective supports, while with silica, a decrease in acid sites was observed after cesium deposition (Table 1). CsO species on the support centers act as electron attractor centers creating Lewis like Cs species. The TiO_2-anatase supports, if pure only show Lewis acidity, whereas in presence of water, Cs—O—H is formed. [43].

4.7. Mechanism of the reaction

The ozonation of organic compounds involves a number of complex reactions and many approaches have been presented in the literature [44]. It is widely accepted that ozone reacts in aqueous solutions containing various organic or inorganic compounds, either by direct reaction of molecular ozone or through

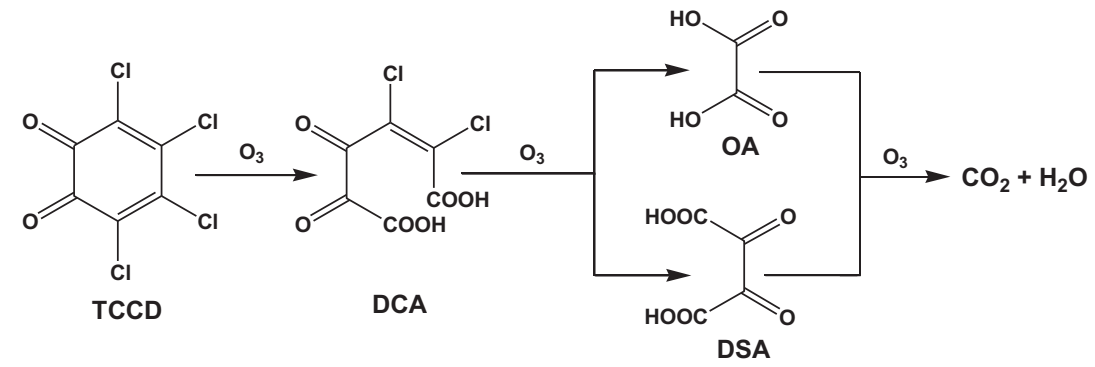

Proposed Mechanism:

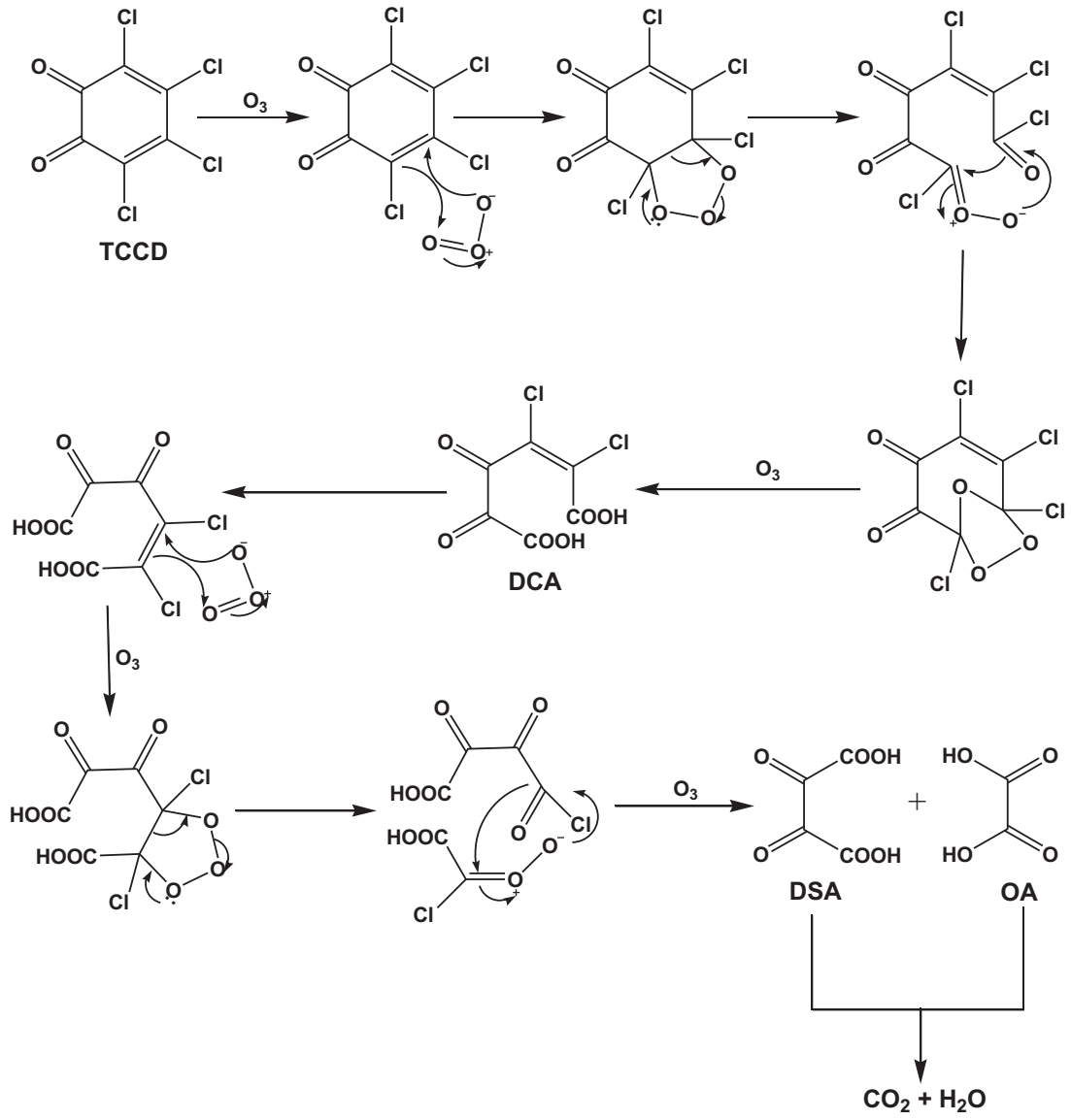

Scheme 1. 3,4,5,6-Tetrachlorocyclohexa-3,5-diene-1,2-dione (TCCD); 2,3-Dichloro-4,5-dioxohex-2-enedioic acid (DCA), Dioxosuccinic acid (DSA) and Oxalic acid (OA). Proposed Mechanism: Mechanism of the Scheme.

a radical type reaction involving HO• radicals resultant from the decomposition of ozone in water. In heterogeneous catalytic ozonation, it is generally assumed that both surface and liquid bulk reactions can occur, involving molecular ozone, HO• radicals and surface oxygenated radical species [44,45]. In general, the proposed mechanisms of ozonation catalyzed by metal oxides assume that the adsorption of organic molecules and ozone takes place on the surface of the catalyst [46]. Ozone interaction with the metal oxide surface results in the formation of free radicals that can initiate a radical chain type reaction both on the surface of the catalyst

and in the liquid phase, leading to the production of HO• radicals [47].

Effective ozonation at pH 7 could possibly be explained by the fact that the products which are formed as a result of degradation as well as the parent compound itself are attacked simultaneously, both becoming important scavengers of hydroxyl radicals [48]. The efficiency of the catalytic ozonation process depends to a great extent on the catalyst and its surface properties as well as the pH of the solution that influences the properties of the surface active sites and ozone decomposition reactions in aqueous solutions [49].

In the proposed mechanism for TCCD ozonation, ozone due to its electrophilic character commonly reacts with aromatic rings by electrophilic substitution [50]. Thus, similar ozonation mechanisms are expected in the case of TCCD oxidation. The reaction pathways proposed in Scheme 1 explains the formation of major transformation products, DCA, DSA and OA. 3,4,5,6-tetrachlorocyclohexa-3,5-diene-1,2-dione (TCCD) possessing electron withdrawing groups will be less reactive and ozone molecule attacks mainly on the least deactivated position, leading to the formation of ozonide intermediate, which gets further oxidized. Ozonide is generated and added to the C=C double bond. The hydroxyl radicals (•OH) generated in the system attack the reaction intermediates to form partially oxidized product, 3-dichloro-4,5-dioxohex-2-enedioic acid (DCA). On oxidation, DCA leads to formation of 2,3-dioxosuccinic acid (DSA) and oxalic acid (OA).

5. Conclusions

In this work, we reported the transformation products arising from TCCD oxidation with ozone with conversions and selectivity and probable mechanism is described. 2,3-dichloro-4,5-dioxohex-2-enedioic acid (DCA) is the main product and 2,3-dioxosuccinic acid (DSA) and oxalic acid (OA) were secondary oxidation products. All the reactions products were dechlorinated ones, and further oxidation gave mineralized products, CO_2 and water. Metal oxide supported Cs catalysts are found to have good product selectivity for partial oxidation to DSA in water at pH 7. While the conversion efficiency of the support was $TiO_2 > Al_2O_3 > SiO_2$, for 0.5 ozone molar ratio, 1% Cs loaded catalysts registered lower conversion than with 5% loaded.

Acknowledgements

Authors thank the University of KwaZulu-Natal for the financial support and other research facilities.

Appendix A. entry data

Supplementary data associated with this article can be found, in the online version, at http://dx.doi.org/10.1016/j.apcatb.2013.02.017.

References

[1] C. Cooper, R. Burch, Water Research 33 (1999) 3695–3700.
[2] R.J. Miltner, H.M. Shukairy, R.S. Summers, Journal of the American Water Works Association 84 (1992) 53–62.
[3] U. Iriarte, J.I. Alvarez-Uriarte, R. Lopez-Fonseca, J.R. Gonzelez-Velasco, Environmental Chemistry Letters 1 (2003) 57–61.
[4] M.D. la Grega, P.L. Buckingham, J.C. Evans, Hazardous Waste Management, McGraw-Hill, New York, 1994.
[5] K.De. Asim, B. Chaudhuri, S. Bhattacharjee, B.K. Dutta, Journal of Hazardous Materials 64 (1999) 91–104.
[6] K. Deweerd, D. Bedard, Environmental Science & Technology 33 (1999) 2057–2063.
[7] B. Peng, H. Zheng-Yi, W. Xin-Jun, C. Jian, B. Yu-Xin, H. Jing, Z. Chun-You, Z. Min, W. Chun-Yan, Environmental Pollution 162 (2012) 303–310.
[8] B. Langlais, D.A. Reckhow, D.R. Brink, Ozone in Water Treatment, Applications and Engineering, Lewis Publishers, Inc., Chelsea, MI, 1991, pp. 569–584.
[9] M. Manassis, S. Constantinos, Ozone Science & Engineering 25 (2003) 167–175.
[10] S.D. Richardson, A.D. Thruston, T.V. Caughran, P.H. Chen, T.W. Collette, K.M. Schenck, B.W. Lykins, C. Rav-acha Jr., V. Glezer, Water, Air, & Soil Pollution 123 (2000) 95–102.
[11] U. Von Gunten, Water Research 37 (2003) 1469–1487.
[12] W.H. Glaze, H.S. Weinberg, Identification and Occurrence of Ozonation By-Products in Drinking Water, American Water Works Association Research Foundation, Denver, CO, 1993.
[13] W.R. Haag, J. Hoigne, Environmental Science and Technology 17 (1983) 261–267.
[14] S.D. Richardson, A.D. Thruston Jr., T.V. Caughran, P.H. Chen, T.W. Collette, T.L. Floyd, K.M. Schenck, B.W. Lykins Jr., G.-R. Sun, G. Majetich, Environmental Science and Technology 33 (1999) 3378–3383.
[15] S.D. Richardson, Disinfection by-products: formation and occurrence of drinking water, in: J.O. Nriagu (Ed.), The Encyclopedia of Environmental Health, 2, Elsevier, Burlington, 2011, pp. 110–136.
[16] E. Gilbert, Water Research 22 (1988) 123–126.
[17] G. Marci, E. Garcia-Lopez, L. Palmisano, Journal of Applied Electrochemistry 38 (2008) 1029–1033.
[18] M.K. Ramseier, A. Peter, J. Traber, U. Von Gunten, Water Research 45 (2011) 2002–2010.
[19] W.H. Glaze, Environmental Health Perspectives 69 (1986) 151–157.
[20] J.H. Larsen, M. Lee, P.C. Frost, G.A. Lamberti, D.M. Lodge, Environmental Toxicology & Chemistry 27 (2004) 676–681.
[21] A.N. Pisarenko, B.D. Stanford, D. Yan, D. Gerrity, S.A. Snyder, Water Research 46 (2012) 316–326.
[22] H. Fujita, J. Izumi, M. Sagehashi, T. Fujii, A. Sakoda, Water Research 38 (2004) 166–172.
[23] X. Zhai, Z. Chen, S. Zhao, H. Wang, L. Yang, Journal of Environmental Science 22 (2010) 1527–1533.
[24] M.D. Amiridis, R.V. Duevel, I.E. Wachs, Applied Catalysis B: Environmental 20 (1999) 111–122.
[25] K. Rakness, G. Gordon, B. Langlais, W. Masschelein, N. Matsumoto, Y. Richard, C.M. Robson, I. Somiya, Ozone Science and Engineering 8 (1996) 209–229.
[26] H. Einaga, S. Futamura, Journal of Catalysis 227 (2004) 304–312.
[27] A. Rahman, V.S.R. Pullabhotla, S.B. Jonnalagadda, Catalysis Communications 9 (2008) 2417–2421.
[28] E.C. Chetty, S. Maddila, V.B. Dasireddy, S.B. Jonnalagadda, Applied Catalysis B: Environmental 117–118 (2012) 18–28.
[29] V.B. Dasireddy, S. Singh, H.B. Friedrich, Applied Catalysis A-General 421–422 (2012) 58–69.
[30] T. Hida, K. Komura, Y. Sugi, Bulletin of the Chemical Society of Japan 84 (2011) 960–967.
[31] R.A. Nyquist, R.O. Kagel, Infrared Spectra of Inorganic Compounds, 135, Academic Press Inc., London, 1971, pp. 209–217.
[32] K. Nakamoto, Infrared Spectra of Inorganic and Coordination Compounds, 2nd edn., John Wiley and Sons, New York, 1990.
[33] B. Rajaram, B.B. Tope, T.K. Das, S.G. Hegde, S. Sivasanker, Journal of Catalysis 204 (2001) 358–363.
[34] S. Hong, M.S. Lee, S.S. Park, G. Lee, Catalysis Today 87 (2003) 99–105.
[35] D.L. Michelsen, Pretreatment of Textile Dye Concentrations using Fenton's reagent and Ozonation prior to Biodegradation, AATCC book for Papers (1992) 150–165.
[36] R.A. Sheldon, J.K. Kochi, Metal-Catalysed Oxidations of Organic Compounds: Mechanistic Principles and Synthetic Methodology Including Biochemical Processes, Academic Press, New York, 1981, pp. xvii–xix.
[37] F.J. Beltran, J.F. Garcıa-Araya, P.M. Alvarez, Environmental Progress 19 (2000) 28–35.
[38] R. Gerald, Chemosphere 28 (1994) 1447–1454.
[39] A.J. Bard, R. Parsons, J. Jordan (Eds.), Standard Electrode Potentials in Aqueous Solutions, IUPAC, 1, 1985, pp. 1–58.
[40] S.B. Jonnalagadda, P. Dachipally, Journal of Environmental Science and Health 46A (2011) 887–897.
[41] B. Kasprazyk-Hordern, M. Ziolek, J. Nawrocki, Applied Catalysis B: Environmental 46 (2003) 639–669.
[42] V.I. Parvulescu, C. Paun, V. Parvulescu, M. Alifanti, I. Giakoumelou, S. Boghosian, S.B. Rasmussen, K.M. Eriksen, R. Fehrmann, Journal of Catalysis 225 (2004) 24–36.
[43] M. Zamora, T. Lopez, R. Gomez, M. Asomoza, R. Melendrez, Catalysis Today 107–108 (2005) 289.
[44] E.C. Chetty, S. Maddila, C. Southway, S.B. Jonnalagadda, ACS - Industrial & Engineering Chemistry Research 51 (2012) 2864–2873.
[45] S. Singh, S.B. Jonnalagadda, Catalysis Letters 126 (2008) 200–206.
[46] F.P. Logemann, J.H.J. Anne, Water Science and Technology 35 (1997) 353–361.
[47] B. Legube, N.K.V. Leitner, Catalysis Today 53 (1999) 61–64.
[48] D. Vogna, R. Marotta, A. Napolitano, R. Andreozzi, M. Ischia, Water Research 38 (2004) 414–422.
[49] B. Kasprzyk-Hordern, Advances in Colloid and Interface Science 110 (2004) 19–48.
[50] B. Legube, B. Langlais, M. Dore, Progress in Water Technology 12 (1980) 553–570.